

Analytical Methods

Accepted Manuscript



This is an *Accepted Manuscript*, which has been through the Royal Society of Chemistry peer review process and has been accepted for publication.

Accepted Manuscripts are published online shortly after acceptance, before technical editing, formatting and proof reading. Using this free service, authors can make their results available to the community, in citable form, before we publish the edited article. We will replace this *Accepted Manuscript* with the edited and formatted *Advance Article* as soon as it is available.

You can find more information about *Accepted Manuscripts* in the [Information for Authors](#).

Please note that technical editing may introduce minor changes to the text and/or graphics, which may alter content. The journal's standard [Terms & Conditions](#) and the [Ethical guidelines](#) still apply. In no event shall the Royal Society of Chemistry be held responsible for any errors or omissions in this *Accepted Manuscript* or any consequences arising from the use of any information it contains.

1
2
3
4
5
6
7
8
9
10
11
12
13
14
15
16
17
18
19
20
21
22
23
24
25
26
27
28
29
30
31
32
33
34
35
36
37
38
39
40
41
42
43
44
45
46
47
48
49
50
51
52
53
54
55
56
57
58
59
60

Selective recognition and sensing for adenosine triphosphate by label free electrochemistry based on its inclusion with per-6-ammonium- β -cyclodextrin

Ni Yang, Yongfeng Wei,* Xiaofeng Kang*, Zhuoqun Su

(*Key Laboratory of Synthetic and Natural Functional Molecular Chemistry, College of Chemistry & Materials Science, Northwest University, Xi'an 710127, P. R. China. E-mail: kangxf@nwu.edu.cn, weiyfeng@nwu.edu.cn, Fax: +86-029-81535026)

Abstract:

A novel method for selective sensing of ATP was developed using ferrocenecarboxylic acid (FcA) as an electrochemical probe, based on the competitive reaction between ATP (or ADP, AMP) and FcA with Per-6-ammonium- β -cyclodextrin (*p*ABCD).

*p*ABCD has been synthesized in four steps from β -cyclodextrin by an improved method referring to literatures. In the *p*ABCD molecule, the primary hydroxyl groups at position 6 of β -cyclodextrin have been substituted by amino groups. The presence of amino groups increased the binding ability. *p*ABCD showed the strongest binding ability towards the adenosine triphosphate (ATP), due to not only the host-guest inclusion of the cavity of *p*ABCD with the adenosine base but also the positively charged ammonium of *p*ABCD with the phosphate anion moiety.

FcA, as an excellent electroactive probe, can be included in the *p*ABCD cavity and produce a decreased oxidation signal. However when ATP was added to *p*ABCD-FcA system, the oxidation peak currents increased dependently on the concentration of ATP. In this way, *p*ABCD-FcA system can recognize and sense the ATP through the competitive interaction of ATP and FcA with *p*ABCD. The increased signal of FcA with the addition of ATP in FcA-ABCD system was studied by differential pulsed voltammetry (DPV). The inclusion constant of *p*ABCD with FcA, ATP, ADP and AMP have been evaluated with DPV by application of the Langmuir equation $1/\Delta I = 1/\Delta I_{\max} + 1/(kc\Delta I_{\max})$.

Based on these results, under the optimized experimental conditions, the oxidation current of the FcA of the FcA-*p*ABCD system responding to the concentration of ATP, was

1
2
3 linear in the range of 3.12×10^{-7} – 1.68×10^{-6} mol/L, with a correlation coefficient of 0.9978 and
4
5 the detection limit ($S/N = 3$) of 1.43×10^{-7} mol/L. These results demonstrate that this method
6
7 is highly selective and sensitive for determination of ATP.
8

9
10 **Keywords:** Per-6-ammonium- β -cyclodextrin, Adenosine triphosphate, Ferrocenecarboxylic
11 acid, Inclusion complexes, Cyclic voltammetry, Differential pulse voltammetry, Inclusion
12 constant, Competitive interaction
13
14

15 1. Introduction:

16
17 Selective recognition and sensitive detection of ATP is of great significance because
18 ATP is one of the most important metabolites in biological systems to support general cellular
19 works necessary for survival and reproduction¹ and the level of ATP is closely related to
20 variety of common physiological diseases such as cardiovascular disease, Parkinsonism, and
21 Alzheimer's²⁻⁴. Therefore, recently, great efforts have been dedicated to develop effective
22 methods that can selectively recognize and sense nucleotides, especially the three basic
23 anionic adenosine phosphates, AMP, ADP and ATP.
24
25
26
27
28
29
30

31 Nowadays, different techniques have been reported for the determination of ATP, such
32 as fluorescence⁵, UV–Vis reflectance spectrum⁶, high performance liquid chromatography
33 (HPLC)⁷ and electrochemiluminescence (ECL)⁸. Until now, there is fewer electrochemical
34 methods reported to determine ATP due its sluggish electrochemical activity, that is, it is hard
35 to be reduced or oxidized directly on electrodes to produce detectable current signal.
36
37
38
39

40 The development of novel system for indirect recognizing and detecting ATP becomes
41 more crucial. According to the literature, nucleotide sensors consist of the receptor moieties
42 and the signaling units. Existing artificial nucleotide receptors can be classified as the
43 multiple amino compounds, polyammoniums⁹, peptides, dendrimers, metallic complexes, and
44 cyclodextrin derivatives.
45
46
47
48

49 β -cyclodextrin (β -CD), having its special conic structure containing a hydrophobic
50 internal cavity and a hydrophilic external surface^{10,11}, are being explored to be as adaptors to
51 recognize the molecule of interest. Since application of natural β -CD is limited because there
52 only exists weak hydrophobic-bonding interaction with guest molecules. In order to strength
53 the recognition ability and selectivity of β -CD to ATP, based on the knowledge about the
54
55
56
57
58
59
60

1
2
3 binding ability of β -amino-cyclodextrin to phosphate anions and nucleotides reported¹²⁻¹⁶, we
4 synthesized the homogeneous *p*ABCD by substitution of the all the primary hydroxyl groups
5 at position 6 with amino pendant groups. Compared with native β -CD, the *p*ABCD is
6 expected to manifests the combined hydrophobic, hydrogen bonding and electrostatic
7 interaction with guest molecules due to the introduction of the amino groups, which may form
8 a crown of positive charges on the opening of the cavity to recognize the anionic guest
9 feasibly in comparison with unmodified β -CD.
10

11
12
13
14
15
16 In order to investigate the binding ability of homemade *p*ABCD with ATP by
17 electrochemical methods, FcA was employed as a probe to study the binding ability of
18 *p*ABCD to ATP by cyclic voltammetry (CV) and DPV based on the competitive reaction of
19 ATP and FcA with *p*ABCD because FcA is a good electroactive probe¹⁷, which can produce a
20 reversible and sensitive redox CV response in solution, and but also its current signal is
21 affected by the inclusion effect of *p*ABCD.
22
23
24
25
26

27
28 Base on this principle and the pre-research, we investigated about the interaction of the
29 ATP and the *p*ABCD. We found that, when FcA coexist with *p*ABCD in solution, there is
30 steady current signal from the oxidation of free FcA. The signal will increased with the
31 addition of ATP due to the competitive binding of ATP and FcA with *p*ABCD and more free
32 FcA expelled out from the cavity. Under the optimal experimental conditions, the oxidation
33 current of the FcA in the FcA-*p*ABCD system responds to the concentration of ATP. As well,
34 these results demonstrated the developed method is selective and highly sensitive for
35 determination of adenosine disodium triphosphate. The mechanism was also proposed based
36 the comparison of inclusion effect of ATP with β -CD and *p*ABCD, *p*ABCD with ATP, ADP
37 and AMP, HPO_4^{2-} and AMP with *p*ABCD. The results show, the *p*ABCD can recognize ATP
38 selectively is due to not only inclusion ability of the hydrophobic cavity and also the electro
39 static attraction between ammonium ions in *p*ABCD and phosphate anions in ATP.
40
41
42
43
44
45
46
47
48
49

50 2. Experimental

51 2.1 Reagents

52 β -CD (purchased from Aldrich) was dried at 120 °C overnight under vacuum before use.
53 Adenosine triphosphate was obtained from Sigma-Aldrich (Shanghai, China). DMF was dried
54 over CaCl_2 and distilled. Ferrocenecarboxylic acid and other reagents were purchased from
55
56
57
58
59
60

1
2
3 Aldrich and were of the best commercial quality available. All inorganic salts were analytical
4 grade and used without further purification. All solutions were freshly prepared with Distilled
5 water which was further purified via an E-Pure 4-Holder system (Barnstead).
6
7

8 9 **2.2 Instruments**

10 ^1H and ^{13}C NMR spectra were determined with Varian INOVA-400M spectrometer
11 working at 400 MHz and 100 MHz for ^1H and ^{13}C nucleus, respectively. Chemical shift are
12 given in ppm from tetramethylsilane(TMS) as internal standard. ESI-MS spectra were
13 recorded in a Thermo Finnigan-LTQ-XL spectrometer. Fourier transforms infrared (FT-IR)
14 spectra of each β -cyclodextrin derivatives were recorded with a Bruker TENSOR-27
15 spectrometer between wavenumber of 400-4000 cm^{-1} . The pH measurements were performed
16 on a pHs-3B pH meter (Dazhong, Shanghai, China). Electrochemical measurements were
17 carried out on a CHI660C Electrochemical Workstation (ChenHua Instruments Co.,
18 Shanghai, China). A three-electrode system was used in the experiment with the glassy
19 carbon electrode (GCE, 3 mm in diameter) as the working electrode. A saturated calomel
20 electrode (SCE) and a Pt wire electrode were used as reference and counter electrodes,
21 respectively.
22
23

24 25 **2.3 Preparation of stock solutions**

26 The solution of *p*ABCD (5×10^{-3} mol/L) was prepared by dissolving 0.346 g *p*ABCD of
27 in 50mL water. The solutions of Ferrocenecarboxylic acid (2.50×10^{-3} mol/L) was prepared
28 by dissolving 0.575 g Ferrocenecarboxylic acid in 100mL water. Solutions (0.25 mol/L) of
29 Adenosine disodium triphosphate, adenosine disodium diphosphate and adenosine disodium
30 monophosphate were prepared by dissolving proper amount them in water.
31
32

33 34 **2.4 pretreatment of the GCE**

35 The glassy carbon electrode (GCE) was polished with 0.05 mm alumina slurry and
36 rinsed thoroughly with doubly distilled water between each polishing step. Then, it was
37 washed successively with 1 mol/L H_2SO_4 , acetone and doubly distilled water in an ultrasonic
38 bath. Finally, the electrode was dried in the infrared drying oven.
39
40
41
42
43

44 45 **2.5 Electrochemical measurement**

46 CV and DPV measurements were performed in 8 mL of 0.1 mol/L Tris-HCl (pH 7.0)
47 buffer solution and CV and DPV curves were scanned from -0.2 to 0.8 V. The parameters
48
49
50
51
52
53

1
2
3 were set as following, scan rate 0.1V/s, pulse width 0.2 s, pulse period 0.5 s and pulse
4
5 amplitude of 5 mV.
6

7 **3 Results and Discussion**

8 **3.1 The preparation of *p*ABCD**

9
10 To synthesis *p*ABCD efficiently and economically, an improved method was developed
11 based on the literature¹⁸, the structure (**Scheme 1**) and purity of the target product is
12 characterized by means of ¹HNMR, ¹³CNMR, IR and MS.
13
14
15

16
17 (**Scheme 1**)
18

19 **3.2 The interaction of ferrocenecarboxylic acid with per-6-ammonium-β-cyclodextrin**

20
21 Firstly, the electrochemical behavior of FcA on GCE was studied, and then the inclusion
22 effect of *p*ABCD was investigated by means of CV. FcA exhibited a pair of redox peaks
23 within the potential window from -0.2 to 0.8 V. Separate solutions with a constant
24 concentration of FcA (1.56×10^{-4} mol/L) with different concentration of *p*ABCD were
25 prepared and their CV curves were recorded with CHI660C Electrochemical Station. The
26 results (in **Fig.1**), shown that the CV response of FcA depends upon the concentration of
27 *p*ABCD, the peak currents gradually decreased upon the addition of *p*ABCD, although the
28 concentration of total FcA was kept constant. This is because, in the presence of *p*ABCD, the
29 formation of inclusion complexes of FcA and *p*ABCD lead to the decrease of concentration of
30 free FcA than that of FcA in absence of *p*ABCD in the solution, making the less FcA move to
31 the GCE surface, thus resulting in current signal decrease, which supports for the formation of
32 inclusion complexes between *p*ABCD and FcA.
33
34
35
36
37
38
39
40
41
42

43 The corresponding relationship between the anodic peak current and the concentration of
44 added *p*ABCD are shown in the inset plots. From these figures, the anodic peak currents
45 decrease gradually with the increase of *p*ABCD concentration, and then approach a plateau
46 after the amount of *p*ABCD added was more than 5 times of equivalent of FcA, which
47 implied an almost completion of inclusion of FcA with *p*ABCD.
48
49
50
51

52 (**Fig.1**)
53

54 To study the interaction of the host-guest inclusion further, DPV is also employed to
55 investigate the inclusion constant between FcA with *p*ABCD. As shown in **Fig. 2A**, the
56
57
58
59
60

1
2
3 decreased DPV signals are directly related to the concentration of added *p*ABCD. The
4 inclusion constant has been determined by the Langmuir equation:
5
6

$$1/\Delta I = 1/\Delta I_{\max} + 1/(kc\Delta I_{\max})^{19} \quad (1)$$

7
8 where ΔI is the change of peak current upon the addition of *p*ABCD, ΔI_{\max} is the maximum
9 change of peak current, c is the concentration of *p*ABCD and K is the inclusion constant. The
10 plots of $1/\Delta I$ versus $1/c$ (Inset of **Fig. 2**) were linear ($1/\Delta I$ (μA) = $0.628 + 0.738 (1/c)$ (mM))
11 with a good correlation coefficient of 0.9997. Eq. (1) allows the K were calculated from the
12 ratio of intercept to slope of the double reciprocal curve $1/\Delta I$ versus $1/c$ plot to be 850.5
13 L/mol (283 K)
14
15
16
17
18
19

20
21 (Fig.2)

22 **3.3 The binding of adenosine triphosphate (ATP) and ferrocenecarboxylic acid (FcA)** 23 **with per-6-ammonium- β -cyclodextrin (*p*ABCD)**

24
25 In order to recognize and sense ATP, further investigation was carried out on
26 electrochemical response of ATP to the FcA-*p*ABCD system. Firstly, the solution of $2.5 \times$
27 10^{-6} mol/L *p*ABCD and 5.0×10^{-7} mol/L FcA was prepared and scanned by the DPV method,
28 then after 9.4×10^{-7} mol/L ATP was added the DPV was recorded as well.
29
30
31
32

33 The results shown in **Fig.3**, there is no peak on the DPV curve when only ATP exists or
34 *p*ABCD and ATP coexist in the solution since *p*ABCD and ATP are none electroactive
35 substance. Compared with 5.0×10^{-7} mol/L FcA and 2.5×10^{-6} mol/L *p*ABCD solution
36 without ATP, the peak current increased when ATP solution was added. A conclusion can be
37 drawn, the FcA-*p*ABCD system can response to the addition of ATP, which may be caused
38 by the competitive interaction ATP and FcA with *p*ABCD to expel out more FcA from its
39 *p*ABCD complex (see **Scheme 2**).
40
41
42
43
44
45

46 To compare the binding ability of β -CD, we also repeat the above experiment just using
47 β -CD instead of *p*ABCD. As can be shown in the inset plots, the effect of β -CD either on the
48 oxidative current of FcA or on the binding of ATP is weaker than the *p*ABCD on current. It
49 indicated the *p*ABCD has a stronger binding ability with ATP than β -CD. It inferred that the
50 amino or ammonium group contributed to the effect due to the hydrogen bonding or the static
51 attraction force between the ammonium cations and the ATP phosphate anion.
52
53
54
55
56
57

58 Based on this phenomenon, the *p*ABCD/FcA complex may play as an electrochemical
59
60

probe for the selective sensing of ATP. The selective and sensitive determination methods may be established for sensing of ATP. Therefore the relationship of the rise of the current and the concentration of the ATP added was investigated further.

(Fig.3)

(Scheme 2)

3.4 The interaction of adenosine triphosphate (ATP) with per-6-ammonium- β -cyclodextrin (*p*ABCD)

To get the fundamental data about the binding function of *p*ABCD with ATP, the interaction constant of ATP with *p*ABCD was determined by the DPV using FcA as a probe. As shown in **Fig. 4**, the increased DPV signals are directly related to the concentration of ATP. The plot of $1/\Delta I$ versus $1/c$ (Inset of **Fig. 4**) fits to a linear relationship ($1/\Delta I$ (μA) = $0.717 + 1.196 (1/c)$ (mM)) with correlation coefficient of 0.9987. The interaction constant was calculated from the ratio of intercept to slope of $1/\Delta I$ versus $1/c$ plot to be 599.6 L/mol (283 K). Meanwhile the constant of ADP and AMP with *p*ABCD were also investigated and respectively found to be 255.5 L/mol (283 K) (**Fig. 5**) and 141.1 L/mol (283 K) (**Fig. 6**). It means that, the interaction of *p*ABCD with ATP is much stronger than with ADP or AMP.

(Fig.4)

(Fig.5)

(Fig.6)

3.5 Optimization of the Determination Conditions

Based on the response of FcA-*p*ABCD to the addition of ATP, to achieve the better sensing performance, the experimental parameters such as pH, reaction time, scan rate, have been optimized.

3.5.1 Optimization of the pH

The oxidative signal of FcA was investigated by CV under different pH of 0.1 mol/L Tris-HCl buffer solutions with 0.5×10^{-3} mol/L FcA, 2.5×10^{-3} mol/L *p*ABCD and 2.5×10^{-3} mol/L ATP. As shown in **Fig. 7A**, the peak currents increased with the pH of the buffer solution in the range of 5.0-7.0. Peak current reaches to the maximum at pH = 7.0. However when the pH was further increased, the peak decreased significantly.

At different pH, the response of FcA-*p*ABCD system to addition of ATP also was investigated. The results show, the increase of the peak current due to the same concentration ATP added have something with pH. At pH = 7.0, the increment of oxidative peak current is much more evident.

This is may be explained that the pH effect on the existing forms of FcA and *p*ABCD, further on the binding ability of *p*ABCD to ATP. Since the *pK*_a of FcA is 4.2²⁰, when pH is more than 4.2, the anionic form of FcA is predominant, which benefits the transfer and the oxidation of FcA on electrode. However, if the pH is too large, it doesn't favor to the protonation of amino group in *p*ABCD because the *pK*_a values of the *p*ABCD were found to be 7.0, 7.7, 7.8, 8.4, 9.0, 9.3 and 12.4 from potentiometric titration curves obtained as described by Martell and Motekaitis, a charged form of the *p*ABCD with a value between 6⁺ and 7⁺ is assumed to be present in aqueous solutions at neutral pH = 7.0²¹. To compromise, the 0.1 mol/L Tris-HCl buffer solution of pH = 7.0 was used as the optimal conditions of supporting electrolyte in the following voltammetric determination.

3.5.2 Optimization of the Reaction time

After mixing of particular concentration of ATP with 0.5×10^{-3} mol/L FcA and 2.5×10^{-3} mol/L *p*ABCD for some time, the CV scan was performed and the CV graph was recorded. As can be shown in **Fig. 7B**, the peak current increased significantly with the increase of mixing time at first and then approached a plateau after 40 min. It indicated that when ATP was added, it took some time to interact with *p*ABCD competitively to drive FcA out of the cavity, which is an electroactive probe and produces oxidative signal.

Therefore, an optimum mixing (reaction) time of 40 min was adopted in the following experiments.

(Fig.7)

3.5.3 Optimization of the Scan Rate

The effect of the scan rate for redox peak current was investigated. As shown in **Fig. 8**, the redox peak currents gradually increase when the scan rate in the range from 0.03 to 0.3 V/s. The redox peak currents increase with the scan rates, The relationship between the redox peak current and the square root of scan rate is well fitted to linear equation (Inset **A** of **Fig.8**), and the regression equation are expressed as $i_{pa}(\mu A) = 0.108 + 13.194 v^{1/2}$ (V/s) ($R = 0.9987$)

and $i_{pc} (\mu A) = 0.228 - 11.714 v^{1/2} (V/s)$ ($R = 0.9991$), which suggested that this electrochemical redox processes are diffusion-controlled.

Meanwhile, the relationship between the redox peak potential and the scan rates was also investigated (Inset **B** of **Fig.8**). The redox peak potentials kept constant with the scan rates in the range of 0.03-0.15 V/s. When the scan rate exceeds 0.15 V/s, the reduction peak potentials shift negative, and the oxidation peak potentials shift positive. The redox process becomes a little irreversible, which is not good to the following measurement. Therefore, a scan rate of 0.1 V/s was adopted in the following experiments.

(**Fig.8**)

3.6 Determination of Adenosine triphosphate (ATP)

Under the chosen conditions, solutions with a constant concentration of 2.50×10^{-6} mol/L *p*ABCD and 0.50×10^{-6} mol/L FcA upon the addition of different concentration of ATP were measured by means of DPV measurements. The result was shown in **Fig. 9**, there is a linear relationship between the current and ATP concentration of $3.12 \times 10^{-7} - 1.68 \times 10^{-6}$ mol/L. The regression equation is $\Delta I (nA) = 42.20 + 4.00 c (\mu M)$ with a correlation coefficient of 0.9978 (Inset of **Fig. 9**), and the detection limit of ATP is 1.43×10^{-7} mol/L ($S/N = 3$).

(**Fig.9**)

3.7 Selectivity and Repeatability

The Selectivity of this method was examined by detecting the effect of fourteen potential interference agents: Na^+ , Fe^{3+} , Ca^{2+} , Cu^{2+} , K^+ , NO_3^- , Cl^- , CO_3^{2-} , SO_4^{2-} , PO_4^{3-} , $H_2PO_4^-$, HPO_4^{2-} , AMP, ADP. As shown in **Fig.10**, fourteen interfering agents led to some signal change, in contrast to ATP, the addition of Na^+ , Fe^{3+} , Ca^{2+} , Cu^{2+} , K^+ , NO_3^- , Cl^- , CO_3^{2-} , SO_4^{2-} , PO_4^{3-} , produced less than 1.89% of the peak current produced by the equivalent ATP. So it indicated that their interferences can be negligible. However, equivalent HPO_4^{2-} , AMP, ADP only produce less than about 16.7% of the peak current of ATP.

Meanwhile, the reproducibility of the method was evaluated by detecting the current response of 9.37×10^{-7} mol/L ATP respectively. The relative standard deviation (RSD) is found to be 2.4%, indicating an acceptable accuracy.

3.8 Discussions on the inclusive mechanism of *p*ABCD

Base on the experimental data, a possible mechanism is proposed as Scheme 2. Firstly,

1
2
3 the inclusion effects of natural β -CD (without any amino group) and *p*ABCD with ATP was
4 compared, the inclusion ability of *p*ABCD is stronger than β -CD, it indicates the ammonium
5 cations play an important role in the inclusion process. Secondly, the inclusion effects of
6 *p*ABCD with ATP, ADP and AMP, which have 3, 2 or only 1 phosphate anion(s) is
7 decreasing with number of charge on the basic anionic adenosine phosphates, it implied the
8 electrostatic attraction between negative charges and positive charges on ammoniums play an
9 important role in the inclusion. Thirdly, the inclusion effect of *p*ABCD with HPO_4^{2-} and AMP
10 was also compared, although the same negative charge on both of them, the inclusion effect
11 of *p*ABCD to AMP is stronger than HPO_4^{2-} , it indicated that the base moiety also can be
12 included in the hydrophobic cavity of *p*ABCD⁹.

13
14 In a word, in the inclusion of *p*ABCD with ATP, the inclusive effect of the hydrophobic
15 cavity with the adenosine base group and the electrostatic static attraction between the
16 polyammonium cations and the negatively charged phosphate moieties in the ATP both play a
17 very important synergic effect, which makes the recognition more selectively and the sensing
18 more sensitively.

19
20
21
22
23
24
25
26
27
28
29
30
31
32
33
34
35
36
37
38
39
40
41
42
43
44
45
46
47
48
49
50
51
52
53
54
55
56
57
58
59
60

(Fig.10)

4. Conclusions

Using own synthesized per-6-ammonium- β -cyclodextrin as a receptor and ferrocenecarboxylic acid as an electrochemical probe, the inclusion effect of ATP with *p*ABCD was studied. Based on the result, a selective and sensitive electrochemical sensing method to ATP was developed. This method has the advantage of excellent selectivity, high sensitive, fast detection and excellent reproducibility, which are proved to be a unique method for ATP detection.

Acknowledgements

This work was financially supported by the National Science Foundation of China (21175105, 21375104 and 21327806), and the Specialized Research Fund for the Doctoral Program of Higher Education of China (20126101110015).

Notes

Electronic Supplementary Information (ESI) available: Synthesis and characterization of

1
2
3 the *p*ABCD.
4

5 6 **References**

- 7
8 [1] J. R. Knowles, *Annu. Rev. Biochem.*, 1980, 49, 877-919.
9
10 [2] H. Yokoshiki, M. Sunagawa, T. Seki, N. Sperelakis, *Am. J. Physiol. Cell. Physiol.*, 1998,
11 274, 25-37.
12
13 [3] S. Przedborski, M. Vila, *Clin. Neurosci. Res.*, 2001, 1, 407-418.
14
15 [4] L. Annunziato, G. Pignataro, G. F. Di Renzo, *Pharmacol. Rev.*, 2004, 56, 633-654.
16
17 [5] C. Handumrongkul, J. L. Silva, *J. Food. Sci.*, 1994, 59, 67-69.
18
19 [6] S. Trajkovska, S. Dzhékova-Stojkova, S. Kostovska, *Anal. Chim. Acta.*, 1994, 290,
20 246-248.
21
22 [7] Y. Bai, L. Zelles, I. Scheunert, F. Korte, *Chemosphere.*, 1988, 17, 2461-2470.
23
24 [8] J.M. Ryder, *J. Agric. Food. Chem.*, 1985, 33, 678-680.
25
26 [9] D. Q. Yuan, A. Izuka, M. Fukudome, M. V. Rekharsky, Y. Inoue, K. Fujitaa, *Tetrahedron.*
27 *Lett.*, 2007, 48, 3479-3483.
28
29 [10] M. V. Rekharsky, Y. Inoue, *Chem. Rev.*, 1998, 98, 1875-1918.
30
31 [11] F. Wang, M. G. Khaledi, *Anal. Chem.*, 1996, 68, 3460-3467.
32
33 [12] A. V. Eliseev, H. J. Schneider, *Angew. Chem. Int. Ed. Engl.*, 1993, 32, 1331-1333.
34
35 [13] A. V. Eliseev, H. J. Schneider, *J. Am. Chem. Soc.*, 1994, 116, 6081-6088.
36
37 [14] N. Mourtzis, K. Eliadou, C. Aggelidou, V. Sophianopoulou, I. M. Mavridisa, K.
38 Yannakopoulou, *Org. Biomol. Chem.*, 2007, 5, 125-131.
39
40 [15] S. Menuel, R. E. Duval, D. Cuc, P. Mutzenhardt, A. Marsura, *New. J. Chem.*, 2007, 31,
41 995-1000.
42
43 [16] C. Aggelidou, I. M. Mavridis, K. Yannakopoulou, *Eur. J. Org. Chem.*, 2009, 2009,
44 2299-2305.
45
46 [10] T. Matsue, D.H. Evans, O. Tetsuo, N. Kobayashi, *J. Am. Chem. SOC.*, 1985, 107,
47 3411-3417.
48
49 [18] A. Gadelle, J. Defaye. *Angew. Chem. Int. Ed. Engl.*, 1991, 30, 78-80.
50
51 [19] S. Q. Liu, J.J. Xu, H. Y. Chen, *Colloids. Surf. B. Biointerfaces.*, 2004, 36, 155-158.
52
53
54
55
56
57
58
59
60

1
2
3 [20] T. Matsue, D.H. Evans, O. Tetsuo, N. Kobayashi, J. Am. Chem. Soc., 1985, 107,
4 3411-3417.
5

6
7 [21] L. A. Godínez, J. Lin, M. Muñoz, A.W. Coleman, A.E. Kaifer, Electroanalysis., 1996, 8,
8 1072-1074.
9
10
11
12
13
14
15
16
17
18
19
20
21
22
23
24
25
26
27
28
29
30
31
32
33
34
35
36
37
38
39
40
41
42
43
44
45
46
47
48
49
50
51
52
53
54
55
56
57
58
59
60

Figure captions

Scheme 1. The structure of *p*ABCD.

Scheme 2. The interaction mechanism of ATP and FcA with *p*ABCD

Fig.1. The CV responses for FcA (1.56×10^{-4} mol/L) with different concentration of *p*ABCD: (a) 0.00, (b) 0.16, (c) 0.32, (d) 0.47, (e) 0.63, (f) 0.78, (g) 0.94×10^{-3} mol/L. Inset: The corresponding relationship between the peak current and *p*ABCD the concentration. In 0.1 mol/L Tris-HCl (pH, 7.0) buffer solution.

Fig.2. The DPV responses for FcA (1.56×10^{-4} mol/L) with different concentration of *p*ABCD: (a) 0.00, (b) 0.16, (c) 0.31, (d) 0.47, (e) 0.63, (f) 0.78×10^{-3} mol/L. Inset: The plots of $1/\Delta I$ versus $1/c$.

Fig.3. The CV responses for different CD solutions: 0.94×10^{-6} mol/L ATP + 2.50×10^{-6} mol/L CD (blue curve), 0.50×10^{-6} mol/L FcA + 2.50×10^{-6} mol/L CD (red curve), 0.50×10^{-6} mol/L FcA + 2.50×10^{-6} mol/L CD + 0.94×10^{-6} mol/L ATP (green curve), 0.50×10^{-6} mol/L FcA (black curve). (A) CD = *p*ABCD, (B) CD = the native β -CD

Fig.4. The DPV responses to different concentration of ATP: (a) 0.00, (b) 0.13, (c) 0.50, (d) 1.00, (e) 1.50, (f) 1.68, (g) 2.00×10^{-3} mol/L. Inset: The plots of $1/\Delta I$ versus $1/c$. in 0.1 mol/L Tris-HCl (pH, 7.0) buffer solution containing 0.50×10^{-3} mol/L FcA + 2.50×10^{-3} mol/L *p*ABCD.

Fig.5. The DPV responses to different concentration of ADP: (a) 0.00, (b) 0.13, (c) 0.50, (d) 0.75, (e) 1.00, (f) 1.25, (g) 2.00×10^{-3} mol/L Inset: The plots of $1/\Delta I$ versus $1/c$. in 0.1 mol/L Tris-HCl (pH, 7.0) buffer solution containing 0.50×10^{-3} mol/L FcA + 2.50×10^{-3} mol/L *p*ABCD.

Fig.6. The DPV responses to different concentration of AMP: (a) 0.00, (b) 0.50, (c) 0.56, (d) 1.00, (e) 1.25, (f) 1.50, (g) 1.88×10^{-3} mol/L. Inset: The plots of $1/\Delta I$ versus $1/c$. The experiments have been done in 0.1 mol/L Tris-HCl (pH, 7.0) buffer solution containing 0.50×10^{-3} mol/L FcA + 2.50×10^{-3} mol/L *p*ABCD.

Fig.7. (A) The effect of the pH values on the peak current. (B) The relationship between the

1
2
3 peak current and the reaction time. In Tris-HCl buffer solution containing 0.50×10^{-3}
4 mol/L FcA + 2.50×10^{-3} mol/L *p*ABCD + 2.50×10^{-3} mol/L ATP.
5
6

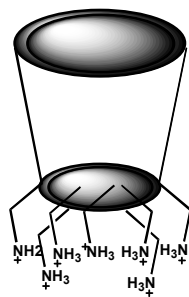
7 Fig.8. The relationship between the peak currents and the scan rates: (a) 0.03, (b) 0.05, (c) 0.10,
8 (d) 0.15, (e) 0.20, (f) 0.25, (g) 0.30 V/s. Inset (A): The linear relationship between the
9 scan rates and the peak currents. Inset (B): The relationship between the logarithm of
10 scan rates and the changes of peak potentials. In Tris-HCl buffer solution containing 0.50
11 $\times 10^{-3}$ mol/L FcA + 2.50×10^{-3} mol/L *p*ABCD + 2.50×10^{-3} mol/L ATP.
12
13
14
15

16 Fig.9. The DPV responses to different concentration of ATP: (a) 0.00, (b) 0.15, (c) 0.30, (d) 1.25,
17 (e) 2.50, (f) 3.75, (g) 7.50, (h)1.00, (i)1.25, (j) 1.68×10^{-6} mol/L. Inset: The corresponding
18 relationship between the anode peak currents and the concentrations. 0.1 mol/L Tris-HCl
19 (pH, 7.0) buffer solution containing 0.50×10^{-6} mol/L FcA + 2.50×10^{-6} mol/L *p*ABCD.
20
21
22
23

24 Fig.10. The increment of peak current(ΔI) in different ions of 0.1 mol/L Tris-HCl (pH 7.0)
25 buffer solution containing 0.50×10^{-6} mol/L FcA + 2.50×10^{-6} mol/L *p*ABCD. ATP
26 (9.37×10^{-7} mol/L) and various ions (1.80×10^{-6} mol/L)
27
28
29
30
31
32
33
34
35
36
37
38
39
40
41
42
43
44
45
46
47
48
49
50
51
52
53
54
55
56
57
58
59
60

1
2
3
4
5
6
7
8
9
10
11
12
13
14
15
16
17
18
19
20
21
22
23
24
25
26
27
28
29
30
31
32
33
34
35
36
37
38
39
40
41
42
43
44
45
46
47
48
49
50
51
52
53
54
55
56
57
58
59
60

Scheme 1.

1
2
3
4
5
6
7
8
9
10
11
12
13
14
15
16
17
18
19
20
21
22
23
24
25
26
27
28
29
30
31
32
33
34
35
36
37
38
39
40
41
42
43
44
45
46
47
48
49
50
51
52
53
54
55
56
57
58
59
60

Scheme 2.

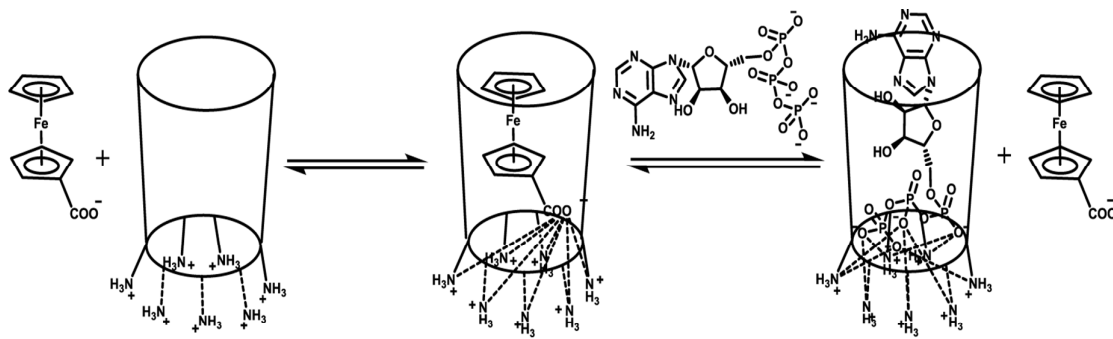


Fig 1 .

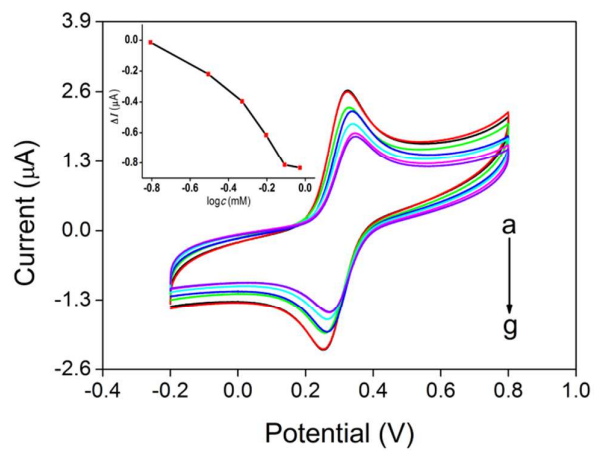
1
2
3
4
5
6
7
8
9
10
11
12
13
14
15
16
17
18
19
20
21
22
23
24
25
26
27
28
29
30
31
32
33
34
35
36
37
38
39
40
41
42
43
44
45
46
47
48
49
50
51
52
53
54
55
56
57
58
59
60

Fig 2.

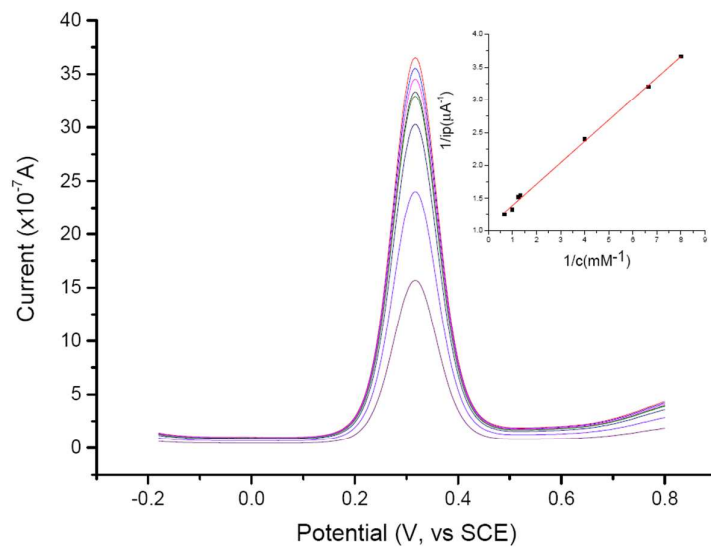


Fig 3.

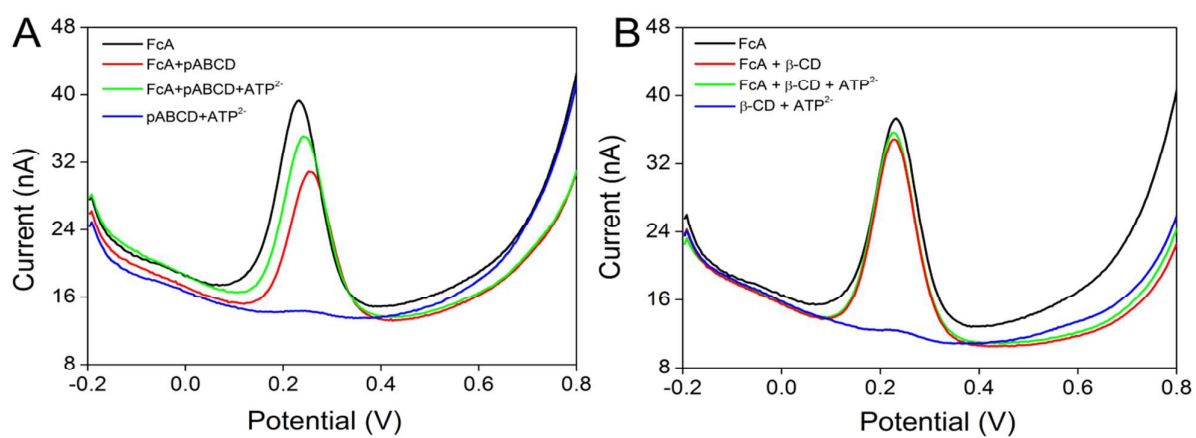


Fig 4.

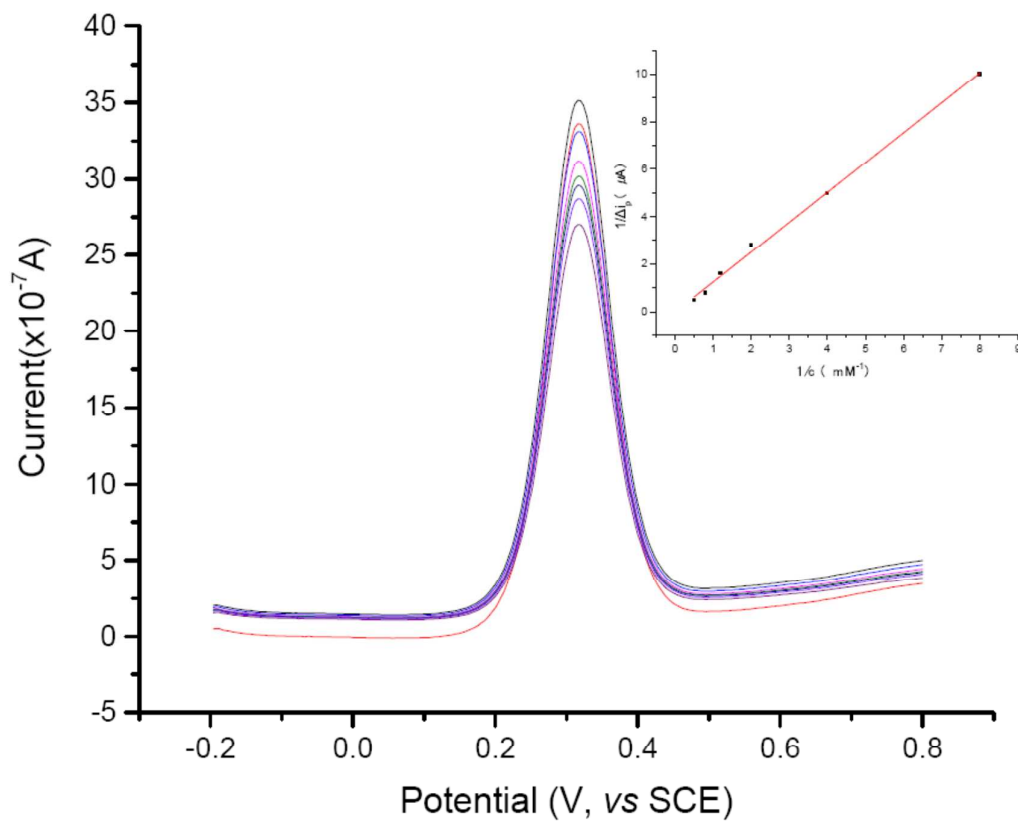


Fig 5.

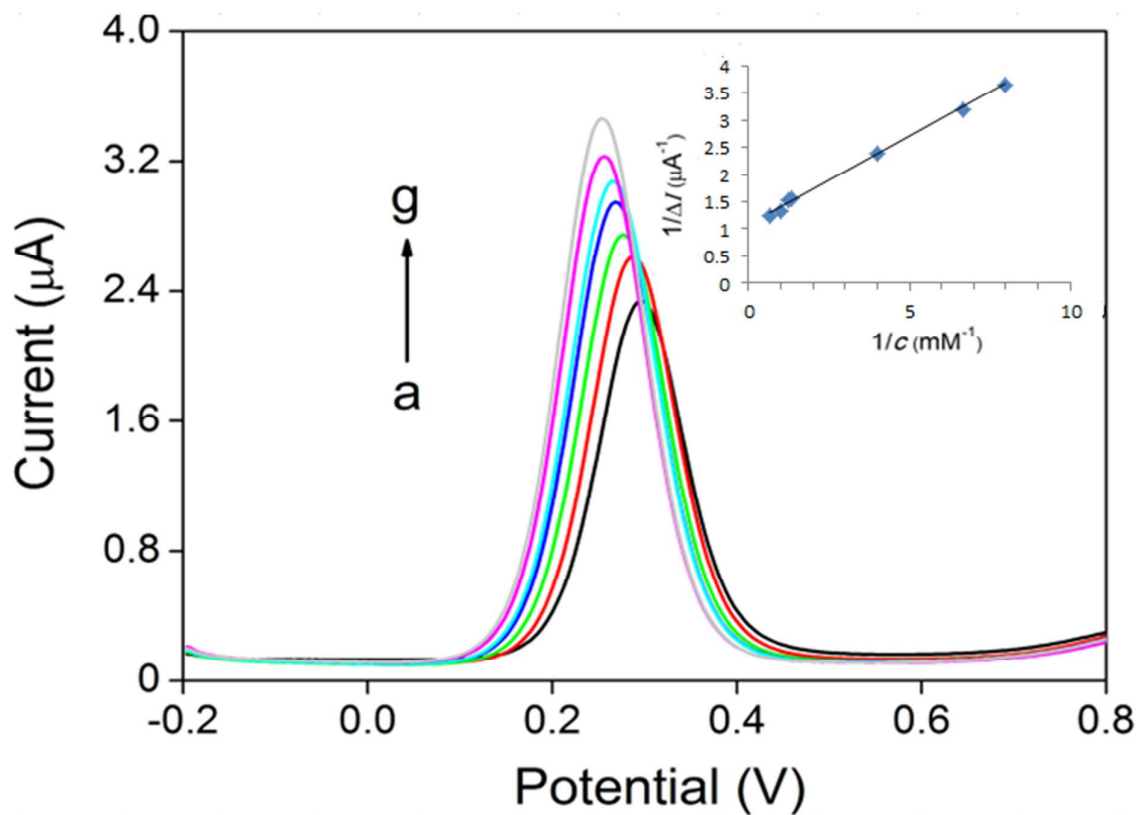


Fig 6.

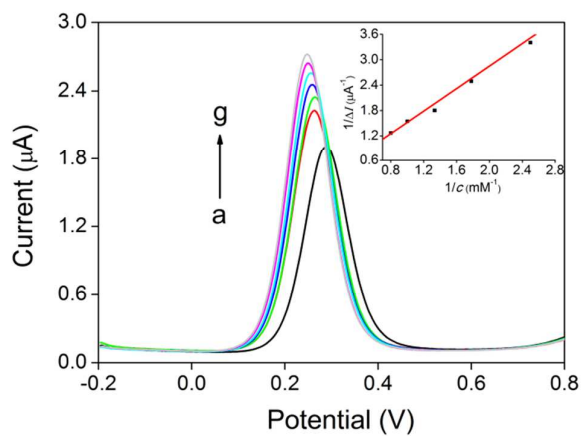
1
2
3
4
5
6
7
8
9
10
11
12
13
14
15
16
17
18
19
20
21
22
23
24
25
26
27
28
29
30
31
32
33
34
35
36
37
38
39
40
41
42
43
44
45
46
47
48
49
50
51
52
53
54
55
56
57
58
59
60

Fig 7.

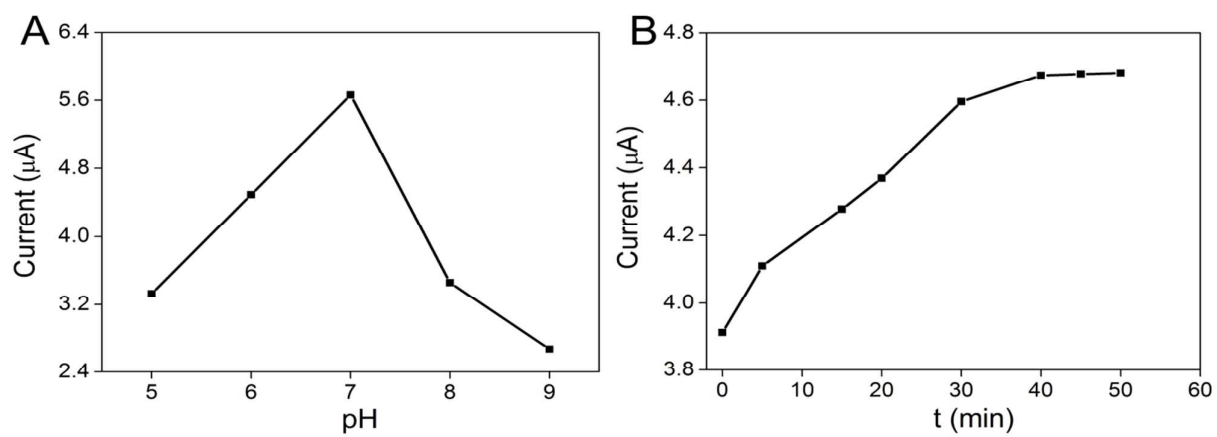


Fig 8.

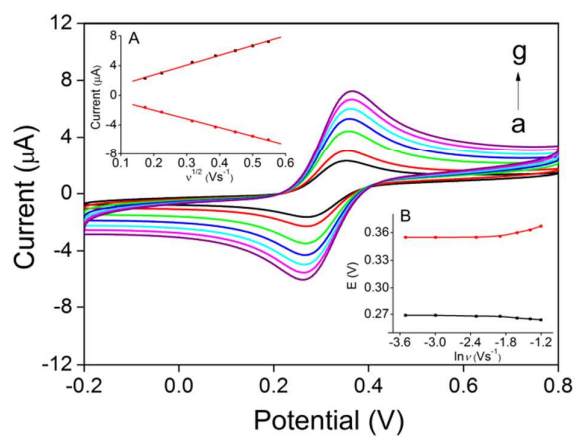


Fig 9.

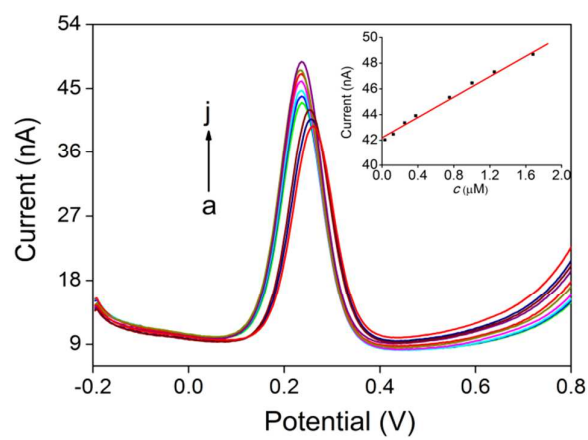
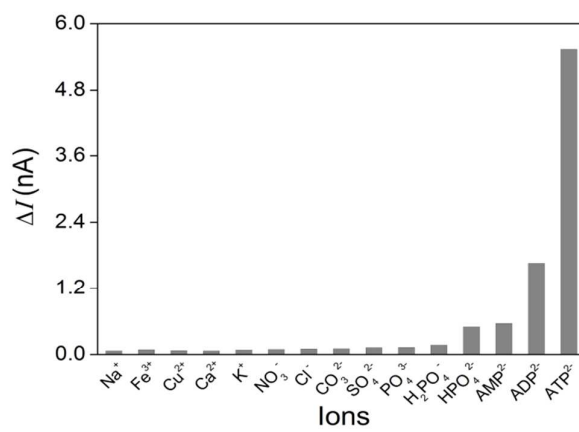
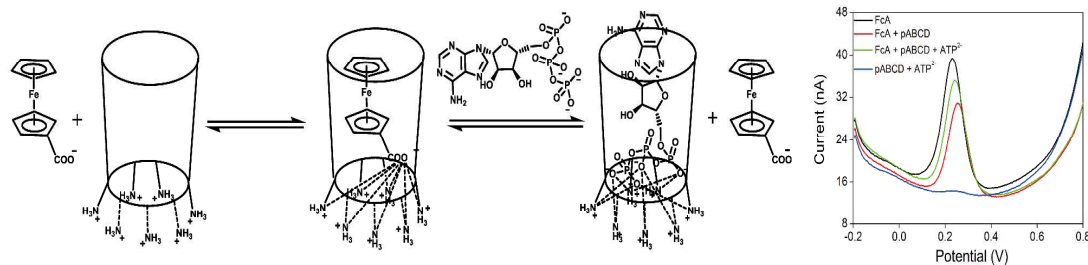
1
2
3
4
5
6
7
8
9
10
11
12
13
14
15
16
17
18
19
20
21
22
23
24
25
26
27
28
29
30
31
32
33
34
35
36
37
38
39
40
41
42
43
44
45
46
47
48
49
50
51
52
53
54
55
56
57
58
59
60

Fig 10.



1
2
3
4
5
6
7
8
9
10
11
12
13
14
15
16
17
18
19
20
21
22
23
24
25
26
27
28
29
30
31
32
33
34
35
36
37
38
39
40
41
42
43
44
45
46
47
48
49
50
51
52
53
54
55
56
57
58
59
60

Graphical Abstract



The illustration diagram for the competitive inclusion of adenosine triphosphate to displace ferrocenecarboxylic acid from its inclusion complex with per-6-ammonium-β-cyclodextrin and the DPV curves.